

Berezinskii–Kosterlitz–Thouless transition of the two-dimensional XY model on the honeycomb lattice

Fu-Jiun Jiang*

Department of Physics, National Taiwan Normal University, 88, Sec.4, Ting-Chou Rd., Taipei 116, Taiwan

The Berezinskii–Kosterlitz–Thouless (BKT) transition of the two-dimensional XY model on the honeycomb lattice is investigated using Neural Network (NN) and Monte Carlo simulations. It is demonstrated in the literature that with certain plausible assumptions, the associated critical temperature $T_{\text{BKT,H}}$ is found to be $\frac{1}{\sqrt{2}}$ exactly. Surprisingly, the value of $T_{\text{BKT,H}}$ obtained from our NN calculations is 0.560(9) which deviates significantly from $\frac{1}{\sqrt{2}}$. In addition, based on the helicity modulus, the $T_{\text{BKT,H}}$ determined is 0.571(8) agreeing well with that resulting from the NN estimation. The outcomes presented in this study indicate that a detailed analytic calculation is desirable to solve the found discrepancy.

I. INTRODUCTION

The two-dimensional (2D) XY model has been one of the research topics in phase transitions. In particular, instead of normal second-order phase transition which is related to spontaneous symmetry breaking, the 2D XY model has a Berezinskii–Kosterlitz–Thouless type transition which is associated with topological defects [1, 2]. Specifically, as the temperature increases, the model exhibits a transition from a phase of bound vortex-antivortex pairs to a phase having unbound vortices and antivortices [3–5]. Such a transition is of infinite order in Ehrenfest’s scheme.

Due to its unique phase transition as well as the relevance to experiments [6–8], the 2D XY model has been studied extensively [9]. In particular, the properties of this model on the square lattice have been determined with high precision. For example, the inverse transition temperature $\beta_{\text{BKT,S}}$ of the 2D XY model on the square lattice is calculated accurately to be 1.1199(1) [10, 11].

During the last decade, one has witnessed an era of applications of Machine Learning (ML) methods in various research fields [12–16]. Moreover, techniques of Neural Networks (NN) have been adopted in uncovering various phases of matters. In particular, NNs are shown to be able to calculate the critical points of many physical models [17–24]. It is worth mentioning that a simple multilayer perceptron (MLP) which has only one hidden layer of two neurons is proved to be universal [25–27], namely the same MLP, without conducting any new training, has been employed to determine the critical temperatures of many three-dimensional (3D) and two-dimensional (2D) models successfully. Apart from this, it is implied in several studies that NN-related approaches may speed up the calculations significantly [28–32]. For instance, it is demonstrated in Ref. [33] that in a Monte Carlo simulation, the configurations obtained much ahead of reaching the equilibrium stage can be employed to identify the critical points of several models with high precision.

By mapping a 2D n -component spin model onto a solid-to-solid model and using certain plausible assumptions, the critical temperature $T_{\text{BKT,H}}$ of the 2D XY model on the honeycomb lattice is found to be $1/\sqrt{2}$ in Ref. [34]. Although $T_{\text{BKT,H}} = 1/\sqrt{2}$ is employed in some later calculations [35, 36], it seems that the result is never confirmed by an exact numerical method. Because of this, here, we apply both the techniques of NN and Monte Carlo simulation (MC) to determine the critical temperature $T_{\text{BKT,H}}$ of the 2D XY model on the honeycomb lattice.

Surprisingly, the NN outcome for the $T_{\text{BKT,H}}$ of the considered model is given by 0.560(9). In addition, by applying the expected finite-size ansatz to the relevant Monte Carlo data, we find that $T_{\text{BKT,H}} = 0.571(8)$. Both the values of $T_{\text{BKT,H}}$, obtained from two different approaches, differ from $1/\sqrt{2}$ significantly. In particular, we find that the estimated pseudo-critical temperatures $T_{\text{BKT,H}}(L)$ is drifting away from $1/\sqrt{2}$ with increasing L .

The critical temperature $T_{\text{BKT,H}}$ of the 2D classical XY model on the honeycomb lattice is determined to be $T_{\text{BKT,H}} \sim 1.1634$ in Ref. [37] by a strong coupling analysis of the two-dimensional $O(N)$ σ model. Later we will argue that the calculations done in Ref. [37] are likely consistent with our results.

In conclusion, the presented results in this investigation indicate that a refinement of the related analytic calculation is required to better understand the deviation between the numerical outcomes reached here and the theoretical prediction of Ref. [34].

*fjjiang@ntnu.edu.tw

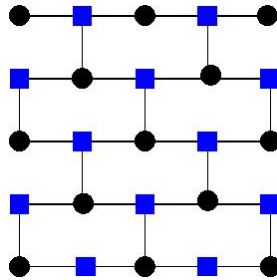


FIG. 1: The periodic 4 by 4 honeycomb lattice implemented in this study.

The rest of the paper is organized as follows. After the introduction, the considered 2D XY model on the honeycomb lattice as well as the calculated observables are described in Sect. II. Moreover, in Sect. III, the employed NN is summarized. We then present the numerical results from both the NN and the Monte Carlo data in Sect. IV. Finally, the conclusions of the present study are given in Sect. V.

II. THE CONSIDERED MODEL AND OBSERVABLE

The Hamiltonian of the 2D XY model considered here has the following expression [11, 38, 39]

$$H = - \sum_{\langle ij \rangle} \vec{e}_i \cdot \vec{e}_j, \quad (1)$$

where $\langle ij \rangle$ refers to the nearest neighbor sites i and j , and \vec{e}_i is a vector at site i with $\vec{e}_i \in S^2$.

Fig. 1 demonstrates the periodic honeycomb lattice implemented in this investigation.

The helicity modulus Γ is calculated here. This quantity describes how the free energy reacts when an infinitesimal change of the boundary conditions is applied to the system. Explicitly, Γ is given by [11, 39]

$$\Gamma = \frac{4}{3\sqrt{3}} \left(\frac{1}{L^2} \left\langle \sum_i^N \vec{e}_i \cdot \vec{e}_{i+1} \right\rangle - \frac{1}{TL^2} \left\langle \left(\sum_i^N (e_i^1 e_{i+1}^2 - e_i^2 e_{i+1}^1)^2 \right) \right\rangle \right). \quad (2)$$

Here T and L are the temperatures and the linear system size ($N = L^2$), and we assume that at the boundaries the twist is applied in the x -direction. The factor $\frac{4}{3\sqrt{3}}$ appearing above is the ratio of the spin densities on the honeycomb and the square lattices.

III. THE NUMERICAL RESULTS

The Monte Carlo simulations (MC) required to calculate the considered critical point $T_{\text{BKT,H}}$ of the 2D XY model on the honeycomb lattice is conducted using the Wolff algorithm [40].

A. The employed MLP

The NN used here is directly adopted from Refs. [41, 42]. The detailed descriptions regarding the construction of the NN are outlined in Refs. [41, 42]. Here for completeness, we briefly introduce the NN used in this investigation as well as the associated training procedure.

The considered NN consists of one input layer, one hidden layer of 512 neurons, and one output layer (no training is carried out in the present study). The algorithm employed is minibatch and the optimizer considered is adam. L_2 regularization is used in the NN calculations to avoid overfitting. In the NN architecture, activations functions ReLU and softmax are applied. 800 epochs are performed and the batch size is 40. Fig. 2 is the cartoon representation for the described NN [41, 42].

The training set for the NN consists of 200 copies of two artificially made configurations. Each of the configurations has 200 elements. In particular, all the elements of the first and the second configurations have the value of 1 and 0,

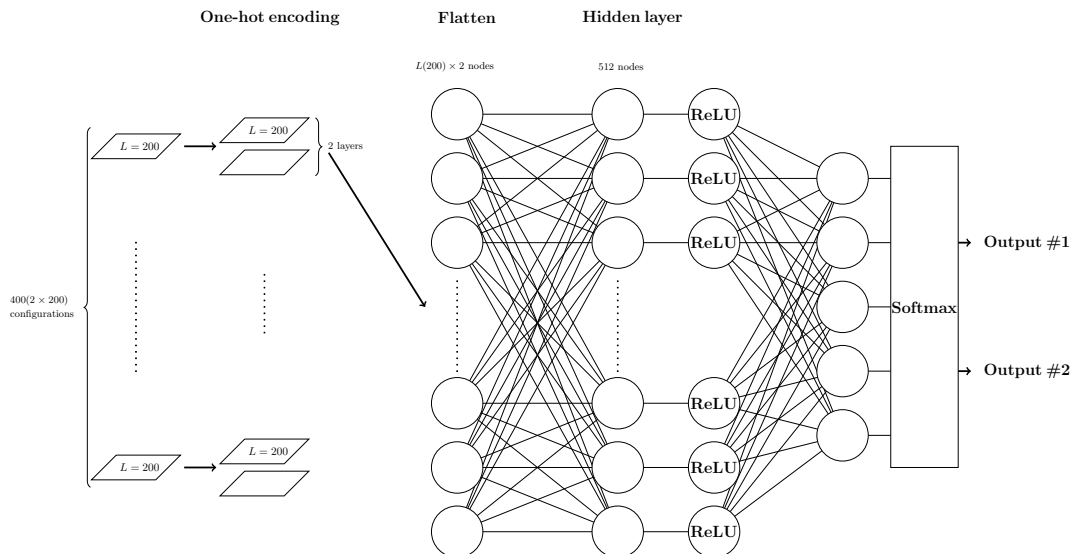


FIG. 2: The MLP employed in this study [41, 42].

respectively. The labels used for these two types of training objects are (1,0) and (0,1). It is demonstrated that the NN with such a training strategy is capable of determining the critical points of several systems [27, 41, 42].

Finally, 10 sets of random seeds are used in our calculations. Therefore there will be 10 NN outcomes. The results presented in the following subsections are based on these 10 NN outcomes.

B. The $T_{\text{BKT,H}}$ of the 2D XY model on the honeycomb lattice determined by the NN method

In this study, the magnitude of the NN output vectors, denoted by R , will be used to determine the critical temperature $T_{\text{BKT,H}}$ of the considered 2D XY model on the honeycomb lattice. Since each of the two types of configurations used in the training set has 200 elements, the required configurations for the NN prediction should have 200 spins. Hence, the configurations for the NN prediction are constructed from the raw spin configurations through the following steps. First of all, two hundred spins are chosen randomly. Second, $\phi \bmod \pi$ of these picked spins are employed to build the configurations for the NN prediction. A typical configuration after the modulus π step has the form $(1,1,0,1,0,0,0,1,\dots,0,0,1)$.

If a configuration is obtained at the high-temperature region, the vortices and anti-vortices are not bound. In addition, the distribution of these topological objects is random and has no specific pattern. As a result, the angles of the spins are random as well. This would lead to a configuration in which the associated elements are arbitrary in 1 and 0 after the mod π step. The output vector of such a configuration is $\sim (0.5,0.5)$ which has $R \sim 1/\sqrt{2}$. The left panel of fig. 3 is a snapshot of a configuration obtained at a high temperature. As can be seen from the figure, the distribution of the angles is quite random. The right panel of fig. 3 shows the result after the mod π procedure for a typical configuration at the high-temperature region. The outcome indeed demonstrates the arbitrariness of the distribution of 1 and 0.

Interestingly, at extremely low temperatures, the majority of the raw spin configurations have one common feature, namely the associated spins' angles $\theta s'$ satisfy either $\theta s' < \pi$ or $\theta s' > \pi$, see the left panel of fig. 4 for a typical snapshot of this described scenario. The right panel of fig. 4 is a representative snapshot after the modulus π step for a configuration in the extremely low-temperature region. The characteristic described above for configurations in the extremely low-temperature region will lead to output vectors around (1,0) or (0,1) which have $R \sim 1$. In conclusion, as one goes from the (extremely) low-temperature region to the high-temperature region, the value of R changes from 1 to a number close to $1/\sqrt{2}$. As we will demonstrate immediately, this is indeed what's been observed.

R as functions of T for $L = 64$ and 128 are shown in the left and the right panels of fig. 5, respectively. Both panels of fig. 5 indicate that as one goes from the low-temperature region to the high-temperature region, the value of R changes from 1 to a number close to $1/\sqrt{2}$.

To calculate the critical temperature $T_{\text{BKT,H}}$, we employ the method used in Ref. [27]. Specifically, for a given L , when the associated R is considered as a function of T , the temperature corresponding to the intersection of R and $(1 + 1/\sqrt{2})/2$ is taken as the pseudo-critical temperature $T_{\text{BKT,H}}(L)$ of the given L . The horizontal lines in both

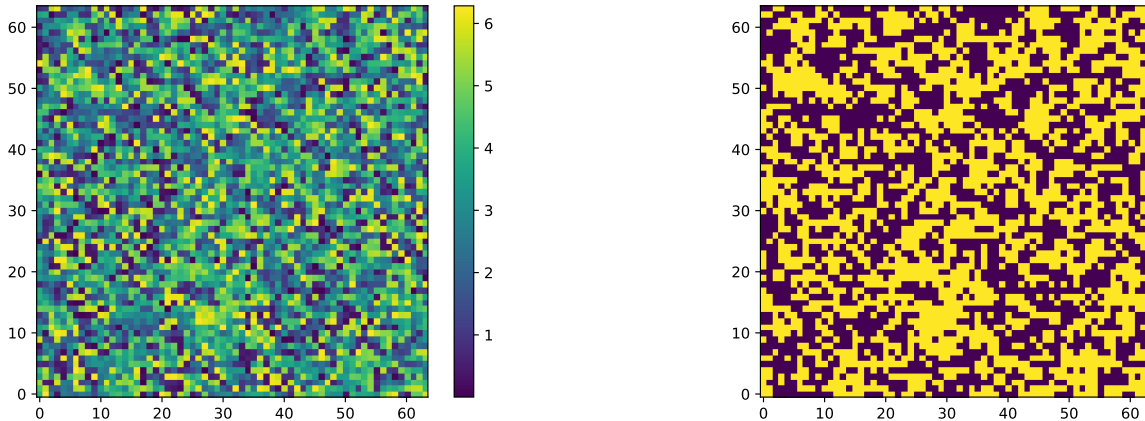


FIG. 3: (Left) The snapshot of a configuration obtained at the high-temperature region. (Right) The result obtained after the mod π procedure for a configuration determined at the high-temperature region.

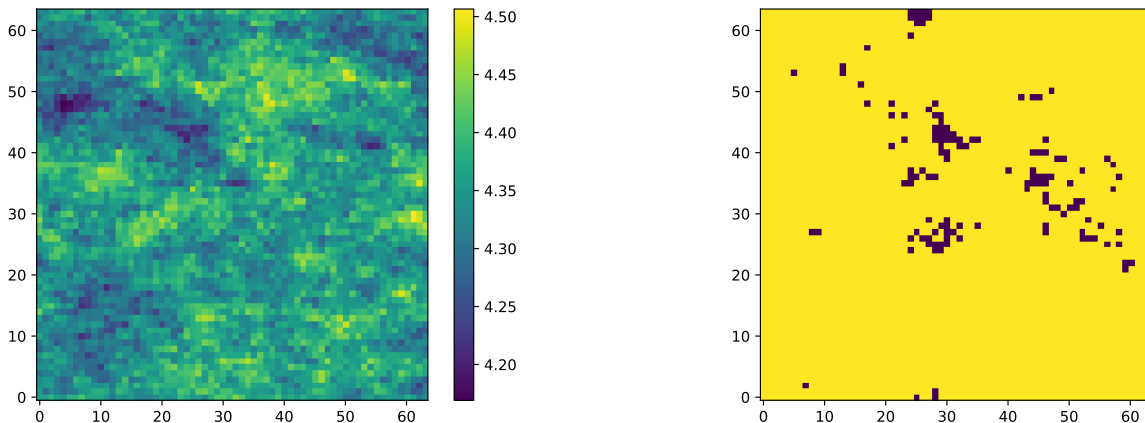


FIG. 4: (Left) The snapshot of a configuration obtained at extremely low-temperature region. (Right) The result obtained after the mod π procedure for a configuration determined at the extremely low-temperature region.

panels of fig. 5 are $(1 + 1/\sqrt{2})/2$.

With the procedure introduced in the previous paragraph, the $T_{\text{BKT,H}}(L)$ as a function of $1/L$ is shown in fig. 6.

Theoretically, it is known that the pseudo-critical temperatures on finite lattices satisfy the following ansatz [43, 44]

$$T_{\text{BKT,H}}(L) = T_{\text{BKT,H}} + a \frac{T_{\text{BKT,H}}}{(\log(L) + c)^2}, \quad (3)$$

where in equation (3) a and c are some constants and $T_{\text{BKT,H}}$ is the bulk critical temperature. A fit of the data in fig. 6 to the above ansatz leads to $T_{\text{BKT,H}} = 0.560(9)$. The obtained $T_{\text{BKT,H}} = 0.560(9)$ deviates significantly from the theoretical prediction $1/\sqrt{2} \sim 0.70711$. As we will show in the next subsection, the $T_{\text{BKT,H}}$ obtained by the NN method agrees well with the one determined from Monte Carlo simulations.

C. The $T_{\text{BKT,H}}$ obtained from the helicity modulus Γ

Fig. 7 shows the helicity modulus Γ of several linear system sizes ($L = 32, 64, 96, 128$) as functions of T . In the figure, the vertical dashed line is $1/\sqrt{2}$ which is the prediction of $T_{\text{BKT,H}}$ from Ref. [34] with certain plausible assumptions. In

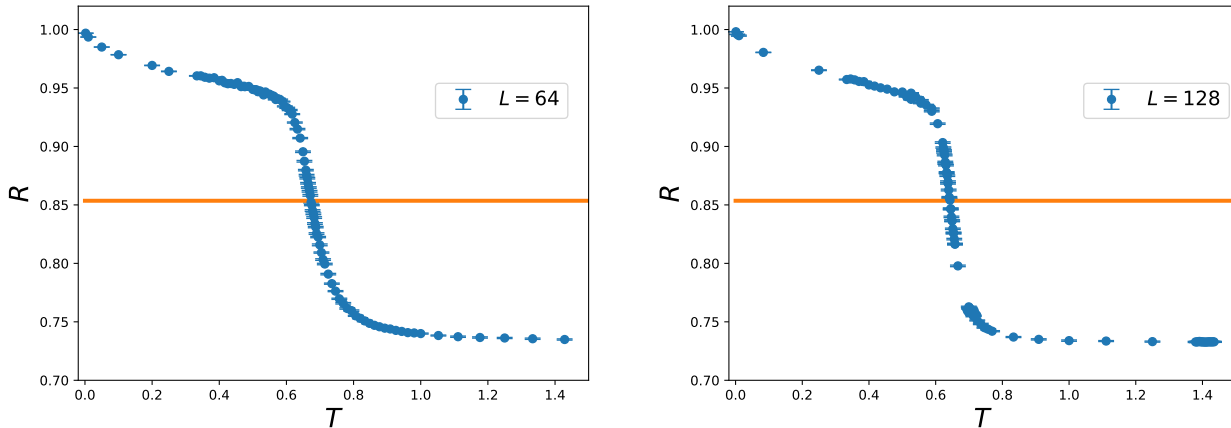


FIG. 5: R as functions of T for $L = 64$ (left panel) and $L = 128$ (right panel). The horizontal solid lines in both panels are $(1 + 1/\sqrt{2})/2$.

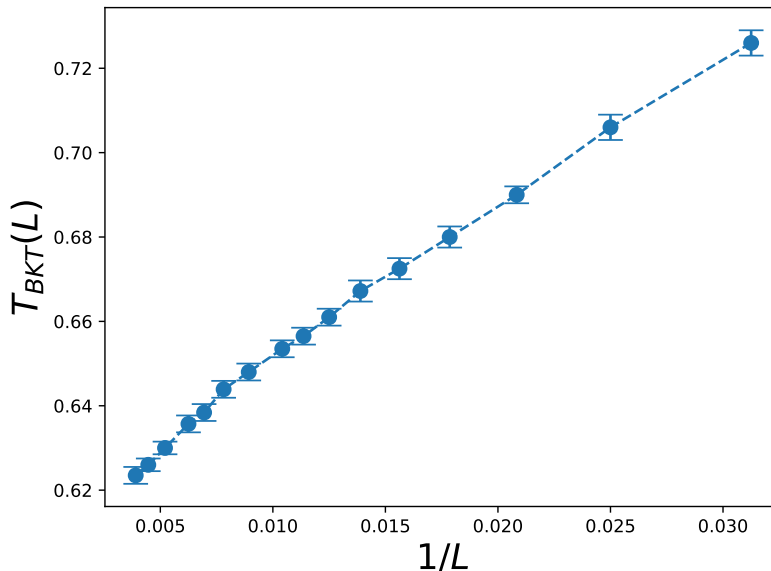


FIG. 6: $T_{\text{BKT,H}}(L)$ as a function of $1/L$. The results are obtained from NN approach.

addition, the solid line in fig. 7 is $2T/\pi$. For each used L , the corresponding $T_{\text{BKT,H}}(L)$ is estimated by the intersection of the associated $\Gamma(L)$ and $2T/\pi$. It is clear that as L increases, the intersection of Γ and $2T/\pi$, namely $T_{\text{BKT,H}}(L)$ drifts away from $1/\sqrt{2} \sim 0.70711$.

$T_{\text{BKT,H}}(L)$ obtained by above described procedure as a function of $1/L$ is demonstrated in fig. 8. A fit using the data of fig. 8 and ansatz (3) leads to $T_{\text{BKT,H}} = 0.571(8)$. In performing the fits, certain reasonable constraints are applied. For instance, only the fits with the results of $T_{\text{BKT,H}} < 1.0$, $c > 0$, and $|a| < 10$ are accepted. It is obvious that the determined $T_{\text{BKT,H}} = 0.571(8)$ agrees with the one obtained by the NN method but differs statistically from the theoretical prediction $1/\sqrt{2} \sim 0.70711$.

IV. DISCUSSIONS AND CONCLUSIONS

Using the NN approach and MC simulations, we calculate the critical temperature $T_{\text{BKT,H}}$ associated with the BKT transition for the 2D XY model on the honeycomb lattice. The obtained outcome $T_{\text{BKT,H}} = 0.560(9)$ and $T_{\text{BKT,H}} = 0.571(8)$ differ significantly from the theoretical prediction $1/\sqrt{2} \sim 0.70711$.

In Ref. [26], the critical temperatures of the associated BKT transitions for the 2D classical 6- and 8-state clock

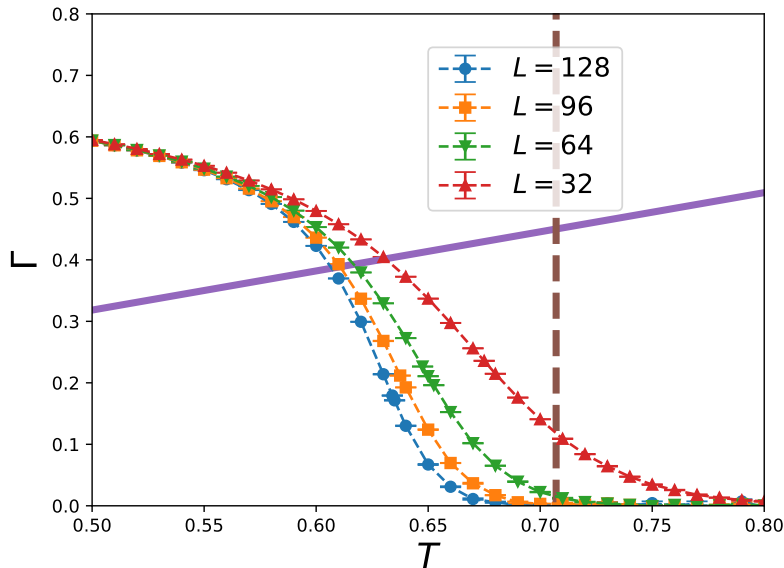


FIG. 7: Intersection points of $2T/\pi$ (solid line) and Γ of various linear box sizes L . The vertical dashed line is $1/\sqrt{2}$ (The predicted critical point from Ref. [34]).

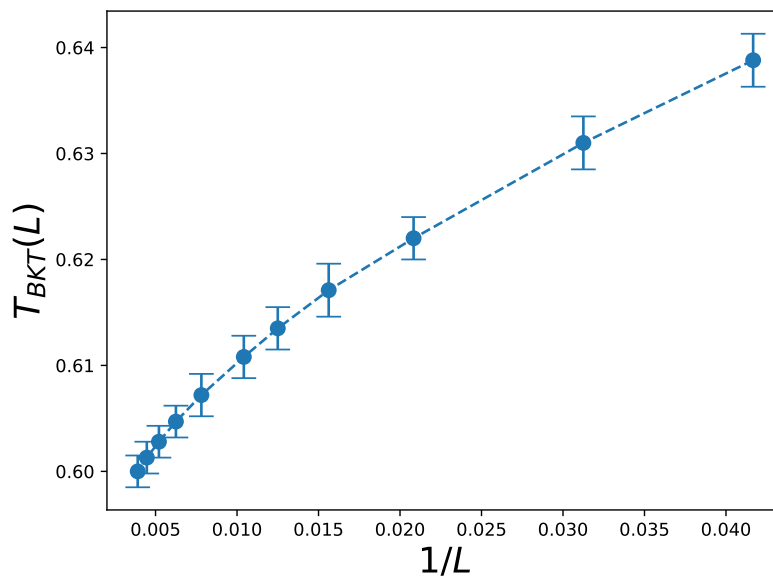


FIG. 8: Pseudo-critical temperatures $T_{\text{BKT,H}}(L)$ as a function of the linear box sizes L . The results are obtained from Γ .

models are calculated. The pseudo-critical temperatures are determined with a method that differs from the one used here. Therefore, one needs to verify that the method employed in this study for calculating the pseudo-critical temperatures is valid for a BKT transition.

Using the data of Ref. [26] as well as the idea of the intersection of R and $(1 + 1/\sqrt{2})/2$, the pseudo-critical temperatures $T_c^1(L)$ associated with the BKT transition from the pseudo-long-range order phase to the paramagnetic phase for the 6-state clock model is shown in fig. 9. With the data of fig. 9 and ansatz (3), one arrives at $T_c^1 = 0.90(2)$ which agrees quantitatively with the known result of $T_c^1 = 0.898(5)$ in the literature [45].

Similarly, with the data of the 8-state clock model from Ref. [26] and the intersection method used here, one arrives at fig. 10 regarding the associated $T_c^1(L)$. A fit of the data in fig. 10 and ansatz (3) leads to $T_c^1 = 0.883(9)$. The obtained $T_c^1 = 0.883(9)$ is in nice agreement with $T_c^1 = 0.8936(7)$ determined in Ref. [46].

The analysis associated with the 6- and 8-state clock models shown above implies the validity of our NN approach

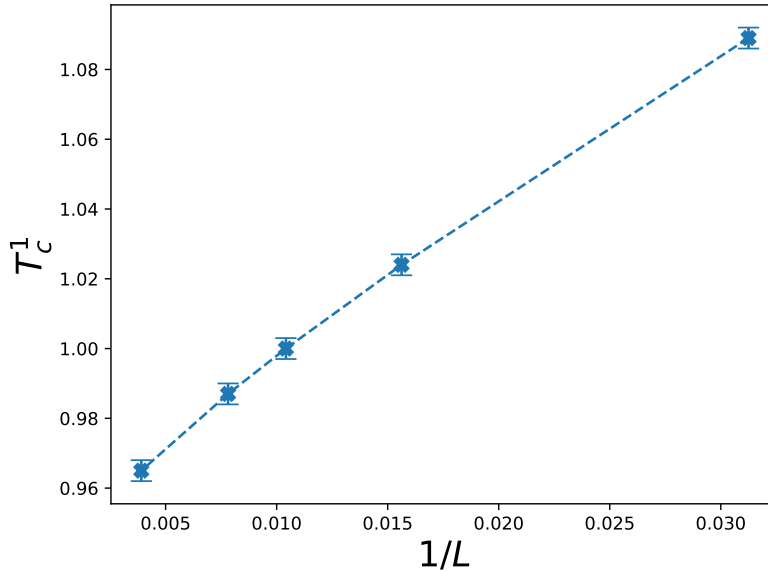


FIG. 9: Pseudo-critical temperatures $T_c^1(L)$ as a function of the linear box sizes L for the 2D classical 6-state clock model.

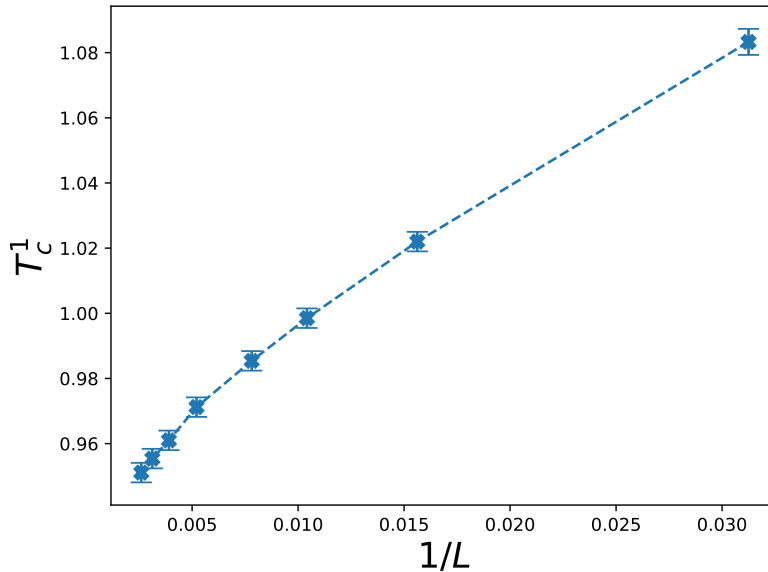


FIG. 10: Pseudo-critical critical temperatures $T_c^1(L)$ as a function of the linear box sizes L for the 2D classical 8-state clock model.

for calculating the critical temperatures of BKT transitions.

In Ref. [37], by the method of strong coupling expansion, the inverse critical temperature $\beta_{\text{BKT,H}}$ of the 2D classical XY model on the honeycomb lattice is found to be $\beta_{\text{BKT,H}} = 0.880$ (This leads to $T_{\text{BKT,H}} = 1.1364$). The $\beta_{\text{BKT,H}} = 0.880$ obtained in Ref. [37] seems inconsistent with both ours and that of Ref. [34]. We would like to emphasize the fact that in Ref. [37] the inverse critical temperature $\beta_{\text{BKT,S}}$ of the 2D XY model on the square lattice is determined to be 0.559 which is only about half of that calculated (by Monte Carlo simulations) in Ref. [11] (The $\beta_{\text{BKT,S}}$ obtained in Ref. [11] is $\beta_{\text{BKT,S}} = 1.1199(1)$). This implies it is likely that one needs to multiply the strong coupling expansion results of Ref. [37] by a factor of 2 to obtain the correct outcomes. If this is true, then the right $\beta_{\text{BKT,H}}$ based on the strong coupling expansion is given by $\beta_{\text{BKT,H}} = 1.76$ with which one arrives at $T_{\text{BKT,H}} = 0.56818$. The conjectured $T_{\text{BKT,H}} = 0.56818$ is in nice agreement with what's reached in this study. It is also worth noticing that while the inverse critical temperature $\beta_{\text{BKT,T}}$ of the 2D XY model on the triangular lattice calculated from

Ref. [37] is 0.340, the $\beta_{\text{BKT,T}}$ estimated from Monte Carlo simulations of Ref. [47] is given by 0.676. Hence, it is of high possibility that the rule of multiplication of factor 2 mentioned above is correct.

It should be pointed out that in Ref. [34], the model used for deriving the critical temperatures of $O(N)$ vector models with $-2 \leq N \leq 2$ is an unphysical one, hence may not capture all the true features of the $O(N)$ universality class. The presented results in this investigation suggest that a refinement of the related analytic calculation is required to better understand the deviation of the numerical outcomes reached here from the theoretical prediction.

Acknowledgement

Partial support from the National Science and Technology Council (NSTC) of Taiwan is acknowledged (NSTC 112-2112-M-003-016-). We thank Jhao-Hong Peng for providing us with some data so that we can verify the correctness of our Monte Carlo code.

-
- [1] V. L. Berezinskii, *Destruction of long-range order in one-dimensional and two-dimensional systems having a continuous symmetry group I. Classical systems*, Sov. Phys. JETP **32** (1971) 493.
 - [2] V. L. Berezinskii, *Destruction of long-range order in one-dimensional and two-dimensional systems possessing a continuous symmetry group II. Quantum systems*, Sov. Phys. JETP **34** (1972) 610.
 - [3] J. M. Kosterlitz and D. J. Thouless, *Long-range order and metastability in two-dimensional solids and superfluids (Application of dislocation theory)*, J. Phys. C **5** (1972) L124. <https://doi.org/10.1088/0022-3719/5/11/002>
 - [4] J. M. Kosterlitz and D. J. Thouless, *Ordering, metastability and phase transitions in two-dimensional systems*, J. Phys. C **6** (1973) 1181-1203. <https://doi.org/10.1088/0022-3719/6/7/010>.
 - [5] J. M. Kosterlitz, *The critical properties of the two-dimensional xy model*, J. Phys. C **7** (1974) 1046-1060. <https://doi.org/10.1088/0022-3719/7/6/005>.
 - [6] D. J. Bishop and J. D. Reppy, *Study of the Superfluid Transition in Two-Dimensional ^4He Films*, Phys. Rev. Lett. **40** (1978) 1727. <https://doi.org/10.1103/PhysRevLett.40.1727>.
 - [7] K. Epstein, A. M. Goldman and A. M. Kadin, *Vortex-Antivortex Pair Dissociation in Two-Dimensional Superconductors* Phys. Rev. Lett. **47** (1981) 534. <https://doi.org/10.1103/PhysRevLett.47.534>.
 - [8] Z. Hu *et al.*, *Evidence of the Berezinskii-Kosterlitz-Thouless phase in a frustrated magnet*, Nat. Commun. **11** (2020) 5631. <https://doi.org/10.1038/s41467-020-19380-x>.
 - [9] J. V. José, *40 Years of Berezinskii-Kosterlitz-Thouless Theory*, World Scientific, 2013. <https://doi.org/10.1142/8572>.
 - [10] M. Hasenbusch and K. Pinn, *Computing the roughening transition of Ising and solid-on-solid models by BCSOS model matching*, 1997 J. Phys. A: Math. Gen. **30** 63. <https://doi.org/10.1088/0305-4470/30/1/006>.
 - [11] Martin Hasenbusch, *The two-dimensional XY model at the transition temperature: a high-precision Monte Carlo study*, 2005 J. Phys. A: Math. Gen. **38** 5869. <https://doi.org/10.1088/0305-4470/38/26/003>.
 - [12] P. Baldi, P. Sadowski and D. Whiteson, *Enhanced Higgs Boson to $\tau^+\tau^-$ Search with Deep Learning*, Phys. Rev. Lett. **114**, 111801 (2015), 1-5. <https://doi.org/10.1103/PhysRevLett.114.111801>.
 - [13] V. Mnih, K. Kavukcuoglu, D. Silver, A. A. Rusu, J. Veness, M. G. Bellemare, A. Graves, M. Riedmiller, A. K. Fidjeland, G. Ostrovski, S. Petersen, C. Beattie, A. Sadik, I. Antonoglou, H. King, D. Kumaran, D. Wierstra, S. Legg and D. Hassabis, *Human-level control through deep reinforcement learning*, Nature **518**, no.7540, 529-533 (2015). <https://doi.org/10.1038/nature14236>.
 - [14] B. Hoyle, *Measuring photometric redshifts using galaxy images and Deep Neural Networks*, Astron. Comput. **16**, 34-40 (2016). <https://doi.org/10.1016/j.ascom.2016.03.006>.
 - [15] Ali Forooghi, Nasim Fallahi, Akbar Alibeigloo, Hosein Forooghi and Saber Rezaey, *Static and thermal instability analysis of embedded functionally graded carbon nanotube-reinforced composite plates based on HSDT via GDQM and validated modeling by neural network*, Mechanics Based Design of Structures and Machines, 51:12, 7149-7182 (2023). <https://doi.org/10.1080/15397734.2022.2094407>.
 - [16] O. Azarniya, A. Forooghi, M. V. Bidhendi, A. Zangoei and S. Naska, *Exploring buckling and post-buckling behavior of incompressible hyperelastic beams through innovative experimental and computational approaches*, Mechanics Based Design of Structures and Machines. <https://doi.org/10.1080/15397734.2023.2242473>.
 - [17] Juan Carrasquilla, Roger G. Melko, *Machine learning phases of matter*, Nature Physics **13**, 431-434 (2017). (2017). <https://doi.org/10.1038/nphys4035>.
 - [18] Evert P.L. van Nieuwenburg, Ye-Hua Liu, Sebastian D. Huber, *Learning phase transitions by confusion*, Nature Physics **13**, 435-439 (2017). <https://doi.org/10.1038/nphys4037>.
 - [19] Dong-Ling Deng, Xiaopeng Li, and S. Das Sarma, *Machine learning topological states*, Phys. Rev. B **96** 195145 (2017), 1-11. <https://doi.org/10.1103/PhysRevB.96.195145>.
 - [20] C.-D. Li, D.-R. Tan, and F.-J. Jiang, *Applications of neural networks to the studies of phase transitions of two-dimensional Potts models*, Annals of Physics, 391 (2018) 312-331. <https://doi.org/10.1016/j.aop.2018.02.018>.

- [21] Kelvin Ch'ng, Nick Vazquez, and Ehsan Khatami, *Unsupervised machine learning account of magnetic transitions in the Hubbard model*, Phys. Rev. E **97**, 013306 (2018), 1-10. <https://doi.org/10.1103/PhysRevE.97.013306>.
- [22] Joaquin F. Rodriguez-Nieva and Mathias S. Scheurer, *Identifying topological order through unsupervised machine learning*, Nat. Phys. **15**, 790–795 (2019). <https://doi.org/10.1038/s41567-019-0512-x>.
- [23] Wanzhou Zhang, Jiayu Liu, and Tzu-Chieh Wei, *Machine learning of phase transitions in the percolation and XY models*, Phys. Rev. E **99**, 032142 (2019), 1-14. <https://doi.org/10.1103/PhysRevE.99.032142>.
- [24] D.-R. Tan *et al.* *A comprehensive neural networks study of the phase transitions of Potts model*, 2020 New J. Phys. **22** 063016, 1-17. <https://doi.org/10.1088/1367-2630/ab8ab4>.
- [25] Jhao-Hong Peng, Yuan-Heng Tseng, Fu-Jiun Jiang, *Machine learning phases of an Abelian gauge theory*, Prog. Theor. Exp. Phys. **2023** 073A03. <https://doi.org/10.1093/ptep/ptad096>.
- [26] Yuan-Heng Tseng, Fu-Jiun Jiang, *Detection of Berezinskii–Kosterlitz–Thouless transitions for the two-dimensional q-state clock models with neural networks*, Eur. Phys. J. Plus, (2023) **138**:1118. <https://doi.org/10.1140/epjp/s13360-023-04741-4>.
- [27] Yuan-Heng Tseng, and Fu-Jiun Jiang, *Learning the phase transitions of two-dimensional Potts model with a pre-trained one-dimensional neural network*, Results in Physics **56** (2024) 107264. <https://doi.org/10.1016/j.rinp.2023.107264>.
- [28] Li Huang and Lei Wang, *Accelerated Monte Carlo simulations with restricted Boltzmann machines*, Phys. Rev. B **95**, 035105 (2017). <https://doi.org/10.1103/PhysRevB.95.035105>.
- [29] Huitao Shen, Junwei Liu, and Liang Fu *Self-learning Monte Carlo with deep neural networks*, Phys. Rev. B **97**, 205140 (2018). <https://doi.org/10.1103/PhysRevB.97.205140>.
- [30] Jan M Pawłowski and Julian M Urban, *Reducing autocorrelation times in lattice simulations with generative adversarial networks*, Mach. Learn.: Sci. Technol. **1** (2020) 045011. <https://doi.org/10.1088/2632-2153/abae73>.
- [31] David Sarrut, Ane Etxebeste, Enrique Muñoz, Nils Kraus and Jean Michel Létang, *Artificial Intelligence for Monte Carlo Simulation in Medical Physics*, Front. Phys. **9**:738112. <https://doi.org/10.3389/fphy.2021.738112>.
- [32] Denny Thaler, Leonard Elezaj, Franz Bamer, and Bernd Markert, *Training Data Selection for Machine Learning-Enhanced Monte Carlo Simulations in Structural Dynamics*, Appl. Sci. **2022**, **12**, 581. <https://doi.org/10.3390/app12020581>.
- [33] Jiawei Ding, Ho-Kin Tang, Wing Chi Yu, *Rapid detection of phase transitions from Monte Carlo samples before equilibrium*, SciPost Phys. **13**, 057 (2022). <https://doi.org/10.21468/SciPostPhys.13.3.057>.
- [34] Bernard Nienhuis, *Exact Critical Point and Critical Exponents of $O(n)$ Models in Two Dimensions*, Phys. Rev. Lett. **49**, 1062 (1982).
- [35] Youjin Deng, Timothy M. Garoni, Wenan Guo, Henk W. J. Blöte, and Alan D. Sokal, *Cluster Simulations of Loop Models on Two-Dimensional Lattices*, Phys. Rev. Lett. **98**, 120601, 2007. <https://doi.org/10.1103/PhysRevLett.98.120601>.
- [36] Jieli Wang, Wanzhou Zhang, Tian Hua, and Tzu-Chieh Wei, *Unsupervised learning of topological phase transitions using the Calinski-Harabaz index*, Phys. Rev. Research **3**, 013074 (2021). <https://doi.org/10.1103/PhysRevResearch.3.013074>.
- [37] Massimo Campostrini, Andrea Pelissetto, Paolo Rossi, and Ettore Vicari, Phys. Rev. B **54**, 7301 (1996). <https://doi.org/10.1103/PhysRevB.54.7301>.
- [38] U. Wolff, Nucl. Phys. B **322** (1989) 759. [https://doi.org/10.1016/0550-3213\(89\)90236-8](https://doi.org/10.1016/0550-3213(89)90236-8).
- [39] Brandon Gómez Bravo, Bryan D. Juárez Hernández, Wolfgang Bietenholz, *Semi-vortices and cluster-vorticity: new concepts in the Berezinskii–Kosterlitz–Thouless phase transition*, Supl. Rev. Mex. Fis. **3** (2022) 020724. <https://doi.org/10.31349/SuplRevMexFis.3.020724>.
- [40] U. Wolff, *Collective Monte Carlo Updating for Spin Systems*, Phys. Rev. Lett. **62**, 361 (1989). <https://doi.org/10.1103/PhysRevLett.62.361>.
- [41] D.-R. Tan, J.-H. Peng, Y.-H. Tseng, F.-J. Jiang, *A universal neural network for learning phases*, Eur. Phys. J. Plus (2021) **136**:1116. <https://doi.org/10.1140/epjp/s13360-021-02121-4>.
- [42] Y.-H. Tseng, F.-J. Jiang, *Berezinskii–Kosterlitz–Thouless transition – A universal neural network study with benchmarks*, Results in Physics **33** (2022) 105134. <https://doi.org/10.1016/j.rinp.2021.105134>.
- [43] D. R. Nelson and J. M. Kosterlitz, *Universal Jump in the Superfluid Density of Two-Dimensional Superfluids*, Phys. Rev. Lett. **39**, 1201 (1977). <https://doi.org/10.1103/PhysRevLett.39.1201>.
- [44] G. Palma, T. Meyer, and R. Labbé, *Finite size scaling in the two-dimensional XY model and generalized universality*, Phys. Rev. E **66**, 026108 (2002). <https://doi.org/10.1103/PhysRevE.66.026108>.
- [45] Tasrief Surungan *et al.*, *Berezinskii–Kosterlitz–Thouless transition on regular and Villain types of q-state clock models*, 2019 J. Phys. A: Math. Theor. **52** 275002. <https://doi.org/10.1088/1751-8121/ab226d>.
- [46] Y. Tomita and Y. Okabe, *Finite-size scaling of correlation ratio and generalized scheme for the probability-changing cluster algorithm*, Phys. Rev. B **66**, 180401(R) (2002), 1-4. <https://doi.org/10.1103/PhysRevB.66.180401>.
- [47] Sun Y-Z, Wu Q, Yang X-L, Zhou Y, Zhu L-Y, Chen Q and An Q, (2022) *Numerical Studies of Vortices and Helicity Modulus in the Two-Dimensional Generalized XY Model*. Front. Phys. **10**:851322. <https://doi.org/10.3389/fphy.2022.851322>.